Environ. Sci. Technol. **2004**, *38,* 5632−5641

Three-Dimensional Dual-Morphotype Species Modeling of Activated Sludge Flocs

ANTÓNIO M. P. MARTINS,† CRISTIAN PICIOREANU, JOSEPH J. HEIJNEN, AND MARK C. M. VAN LOOSDRECHT*
Department of Biotechnology, Delft University of Technology, Julianalaan 67, 2628 BC Delft, The Netherlands

An individual-based model, originally developed for a biofilm system, was adapted to simulate three-dimensional formation of activated sludge flocs. The model was extended to two different bacterial morphotypes (floc-forming and filamentous bacteria), allowing spatial development of the floc according to the bacterial morphology, diffusion, reaction, and growth processes. The model needed also extension with a process for attachment of individual cells. Despite being in an early stage of development, the model is already a tool that enables us to obtain useful information about the microfloc environment. The model indicates that filamentous bacterial morphology and substrate microgradients are important aspects in the formation of bacterial structures. In mass transport-limited regimes filamentous bacterial structures prevail, whereas in growth-limited regimes irregular shaped flocs with fingerlike structures are dominant. These modeling results suggest that activated sludge flocs and biofilms might be different manifestations of the same phenomena. The model results support the hypothesis that floc-macrogradients can be the most important parameter for development of bulking sludge. The model suggests that attachment has a very strong effect on floc structure, leading to enhancement of the effect of substrate microgradients.

Introduction

In microbial aggregates, such as activated sludge flocs, microgradients of electron donor (organic substrate) and/or electron acceptor (e.g., dissolved oxygen) concentrations are ubiquitous. Gradients of substrate concentration (e.g., organic substrates, oxygen, ammonia, nitrite, and nitrate) have been theoretically evaluated and experimentally observed in activated sludge flocs (*1*−*4*). The concentration gradients and their magnitude depend on the ratio between the reaction rate and the mass transfer rate. The specific activity of the bacteria and the density of biomass in the aggregates mainly determine the reaction rate. Mass transfer within the floc depends mainly on diffusional processes and the magnitude of mass transfer limitation depends on the diffusion coefficient, concentration in bulk liquid, and the size of the aggregates. In open porous aggregates convective transport can in certain cases support the diffusional mass transfer. Due to the diffusion, reaction, and growth processes the concentration observed by microorganisms in the aggregate is lower than that in the bulk liquid. This leads to an observed half saturation constant, usually called *apparent half saturation constant*, which is higher than the *intrinsic half saturation constant* for substrate (K_s). In this sense, the apparent K_s can be seen as an apparent mass transfer parameter describing the mass transfer to the cell (*2*, *5*−*7*). Its magnitude depends strongly, for instance, on aggregate morphology. The larger the surface-to-volume ratio of aggregates, or the less dense the structure is (e.g., dominance of filamentous structures), the lower the measured apparent K_s value.

Different values of intrinsic substrate half saturation constant have been used to explain the competition between filamentous and nonfilamentous bacteria in activated sludge flocs (*8*). However, until now no one has unequivocally shown that this mechanism is the true and only one. An alternative hypothesis based on bacterial morphology and diffusion-limited microgradients in activated sludge flocs has been recently developed (*9*−*11*). When the flocs are growing at a low substrate concentration the filamentous bacteria would observe effectively a higher substrate concentration than the floc-forming bacteria inside the floc (*6*, *12*, *13*). Due to their morphology, filamentous bacteria could easily penetrate outside the flocs. Having a predominantly unidirectional growth apparently gives competitive advantages to filamentous bacteria (*9*−*11*). Filamentous bacteria could also serve as a "backbone" for the development of open floc structures (*12*, *14*, *15*). Recent quantitative FISH results that high levels of filaments occurred inside the flocs in nonbulking sludge, supporting this hypothesis for bulking (*16*).

To study complex ecosystems, in which many factors are acting together, mathematical modeling can be a very useful tool. A model can help with the illustration and understanding of what goes on inside the floc, e.g., the penetration depths of the different chemical compounds involved in the process and competition between different species. Modeling has been successfully used to describe the morphology of biofilms developed in gradient governed environments. Incorporating diffusion, reaction, and growth processes in a biofilm model indicated, for instance, that the formation of open and filamentous biofilm structures is stimulated in diffusion dominated conditions (*17*).

Modeling the microenvironment of activated sludge flocs has rarely been reported and even less in bulking sludge studies. Lau et al. (*13*) developed the first bulking sludge mathematical model incorporating simultaneous diffusion of substrates through flocs with predetermined shape and the accompanying growth. Although with several limitations the model illustrates some aspects that may match the reality. For instance, Lau's model predicts that a cylindrical floc has less resistance to substrate diffusion than equal-volume spherical flocs, and therefore the one-dimensional (unidirectional) growth of filamentous bacteria might lead to a floc geometry that is more favorable for substrate diffusion. Later studies combine the morphological characteristics with the physiology of filamentous and nonfilamentous bacteria. Both the micromorphology of the floc and the oriented growth characteristics of filamentous bacteria were taken into account in the mathematical model with preferential unidirectional growth by Takács and Fleit (*18*). However, similar to Lau et al. (*13*), Takács and Fleit (*18*) attributed different kinetic parameters to the two different bacterial morphotypes (filaments and floc-formers). This makes it difficult to differentiate between the role of different substrate half saturation constants and different morphology in the competition between filamentous and nonfilamentous bacteria.

* Corresponding author phone: +31 15-27-81618; fax: +31 15-27-82355; e-mail: M.C.M.vanLoosdrecht@tnw.tudelft.nl.
† Present address: Águas do Algarve, S.A., Direcção de Operações − Saneamento, Rua do Repouso 10, 8000-302 Faro, Portugal.

10.1021/es049659l CCC: $27.50
Published on Web 09/29/2004

Recently, a new modeling approach, named individual-based modeling (IbM), was developed and implemented for biofilm systems (*19*−*22*). IbM allows individual variability and treats bacterial cells as single units. Furthermore, the IbM approach can make a distinction between spreading mechanisms adopted by different bacteria (*21*). The IbM approach contains exceptional features needed to model growth of filamentous bacteria. For example, assuming that filamentous bacteria "remember" a preset growth direction leads to the alignment of "daughter" cells with the "mother" cells in the trichome of the filamentous bacteria. Thus, modeling can be used to evaluate better the role of unidirectional growth of filamentous bacteria in competition with the isotropic growth of floc-forming bacteria. The model is also expected to evaluate the hypothesis that floc-forming bacteria can develop fingerlike structures and fluffy aggregates due to growth in steep substrate gradients combined with attachment of planktonic cells to sludge flocs, under a wide range of kinetic parameters.

The aim of this study is to adapt a previously developed IbM biofilm model and evaluate the model capability to describe structure formation of activated sludge flocs made of two bacterial morphotypes: a filamentous and a non-filamentous microorganism. Diffusion and reaction of soluble substrates, isotropic growth of floc-forming bacteria, and attachment and unidirectional growth of filamentous bacteria are the main processes considered in this model.

Methods

Model Definition. The new floc model, aiming at describing microbial and solute distributions in three spatial dimensions, is an extension of previously reported biofilm models (*17*, *19*, *20*, *22*, *23*). The model simulates the development of a single activated sludge floc contained in a cubical computational domain Ω with the size L (Figure 1). Formation of the biological floc starts with a few initial cells placed in the middle of the cubic domain, which in Cartesian coordinates (x,y,z) are situated around the central point (x_C=$L/2$, y_C=$L/2$, z_C=$L/2$). The computational domain Ω consists of two subdomains, Ω_1 and Ω_2. The *bulk liquid subdomain* Ω_1 is considered completely mixed and therefore of uniform concentration of solutes. The soluble substrate concentrations in the bulk liquid Ω_1 are $C_{S,1}^{(b)}$ and $C_{S,2}^{(b)}$ for oxygen ($g_{O2}\cdot m^{-3}$) and soluble organic substrate ($g_{COD}\cdot m^{-3}$), respectively, which are considered in this study the only essential nutrients. For simplicity, neither biological activity nor other reactions are considered in the bulk liquid. The *diffusional subdomain* Ω_2 contains the biological floc and a spherical mass transfer boundary layer. Therefore, the outer limit of Ω_2 is a spherical surface situated at a distance δ_{BL} from the floc maximum radius R_F, computed as the Euclidian distance between the center of the domain and the outermost biomass particle (Figure 1). Diffusion is the only transport mechanism of solutes within Ω_2.

The multidimensional multispecies floc model developed in this study contained the following key processes:

1. Biomass Growth. It is assumed that the floc consists of two species of active bacteria: the floc-forming and the filamentous microorganisms. Although the particle-based biofilm model (*22*) allowed inert biomass formation as a result of decay processes (Figure 1C), for simplicity, inert production processes were not considered in this study. Thus, cells that do not have access to substrate do not become inactive. The 3-D floc structure is represented by a collection of N_P nonoverlapping hard spheres of biomass, also called biomass particles. Each spherical particle p contains only one type of active biomass (floc-former or filament type, see Point DisplayC). It is assumed that each particle has the total mass $m_X^{(p)}$ (g_{COD}/particle) and a constant density of ρ_X (g_{COD} biomass$\cdot m^{-3}$ particle). When the biomass in the particle changes in time, volume and radius $R^{(p)}$ change accordingly:

$$R^{(p)} = \left(\frac{3m_X^{(p)}}{4\pi\rho_x}\right)^{1/3} \quad (1)$$

The growth of each biomass type b with time is described by an ordinary differential equation representing the mass balance for each biomass particle p:

$$\frac{dm_{X,b}^{(p)}}{dt} r_{X,b} \text{ for each } p = 1,2,...,N_P \text{ and each } b = 1 \text{ (floc-former), 2 (filament)} \quad (2)$$

The net reaction rates for generation of biomass, $r_{X,b}$, are typically functions of the biomass of the particle, $m_{X,b}^{(p)}$, and concentrations $C_{S,n}^{(x,y,z)}$ of various substrates present at the center (x,y,z) of the biomass sphere.

The initial (at time $t = 0$) distribution of biomass particles is in the middle of the cubic domain, i.e., around the point $(L/2,L/2,L/2)$. It is assumed that all $N_{P,0}$ initial biomass particles have mass m_0 and, correspondingly, radius R_0.

2. Biomass Division and Propagation Rules. The bacterial mass contained in each particle will grow according to eq 2. However, the total biomass in a particle is assumed limited to a maximum value, $m_X < M_X$ (g_{COD} biomass $\cdot$ m^{-3} particle), which is independent of growth rate for the sake of simplicity (*18*, *19*). M_X is conveniently chosen to achieve the desired total biomass density in the floc $C_{X,max}$ (g biomass $\cdot$ m^{-3} floc). When this maximum biomass M_X in a sphere is reached, a new "daughter" sphere is created. Part of the biomass contained in the "mother" is redistributed to the "daughter" sphere. To break synchronous divisions from the beginning, an unequal splitting ratio (e.g., by uniformly randomly redistributing between 40 and 60% of the "mother" particle to the "daughter" particle) is prescribed. For floc-forming bacteria, the new "daughter" sphere touches the "mother" sphere in a randomly chosen direction. This isotropic biomass growth mechanism leads to spherical colonies of floc-former bacteria when no growth limitations (e.g., due to diffusion) occur within the colony. Details about the implementation of the isotropic division can be found in refs *19*, *20*, and *22*. A characteristic of this new model is that, as opposed to floc-formers, filamentous bacteria grow in a preferential direction. This preferential direction is kept as an attribute of the filament from the beginning in a pair of spherical coordinates $(\theta,\varphi) = (\theta_0,\varphi_0)$ invariable in time, as opposed to division of floc-formers where the directions (θ,φ) are randomly chosen at each division. The new "daughter" sphere touches the mother sphere, and it is placed in the attributed direction. When the new cell is inserted in the filament, the other cells are pushed in both directions, so that the filament grows on both sides of the floc.

3. Biomass Spreading. The spreading of the floc in space as a result of biomass growth is implemented differently for floc-forming and for filamentous bacteria. For floc-formers, the biomass spreading occurs by shoving the spheres when they get too close to each other. The pressure building up due to floc-formers growth is relaxed by minimizing the overlap of spheres. This mechanism is explained in detail in refs *18*, *19*, and *21*. Similar to the division process, for filamentous bacteria the spreading occurs in a preferential direction, randomly preset. When a new cell is inserted in the filament, the other cells of the trichome are pushed further on the line remembered by all the cells belonging to a filament and defined by the angles (θ_0,φ_0). The spreading floc-formers treat filaments as a rigid wall that effectively bounces them back. However, the spreading filaments can push the floc-former cells being in their way.

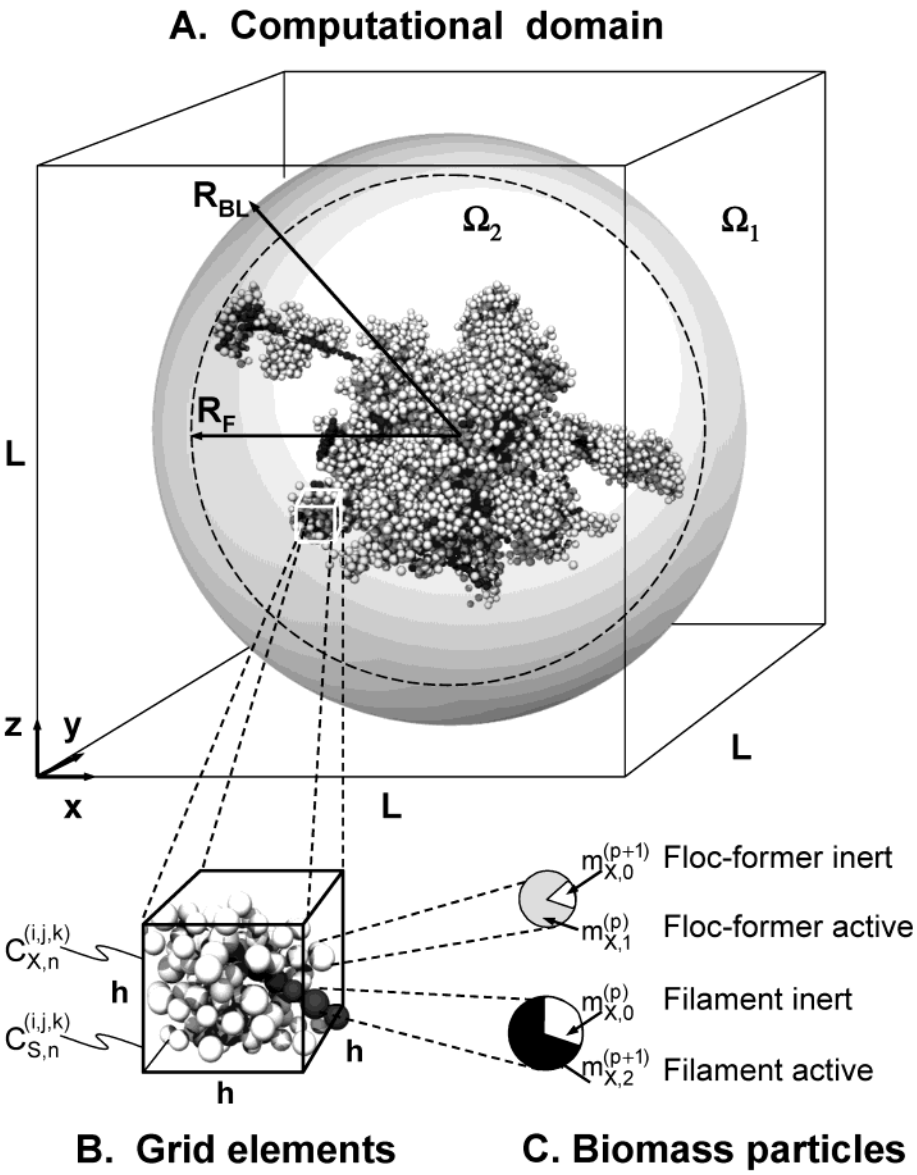

FIGURE 1. The model floc system. (A) The cubic computational domain (3-D) encloses the activated sludge floc. (B) A rectangular uniform grid (mesh size $h=\Delta x=\Delta y=\Delta z$) is used for the solution of the partial differential equations for substrate diffusion and reaction. (C) Biofilm biomass is contained in spherical particles holding one type of active biomass as well as inactive biomass. All biomass particles situated in one grid element *(i,j,k)* experience the same substrate concentrations $C_{S,n}^{(i,j,k)}$. The average biomass concentrations in each grid element are $C_{X,b}^{(i,j,k)}$.

4. Biomass Attachment. Attachment of new biomass particles to the biological floc was considered for both floc-forming and filamentous bacteria. The number of new biomass particles sent into the system to attach in a time interval (Δt) is a fraction f_{att} of the newly formed particles by biomass division in Δt. Consequently, in a sufficiently large time interval, the attachment rate is a fraction f_{att} of the growth rate:

$$r_{X,b}^{(att)} = f_{att,b} \cdot r_{X,b} \tag{3}$$

A ballistic aggregation model (*24*) was used for attachment. Particles were released from an arbitrarily chosen point on a randomly chosen face of the cubic computational domain and let attach to the existing floc after a "random walk" (a kind of Brownian motion ending when the particle touches the floc). The attached filament-forming cells acquire a new preferential growth direction chosen at random.

5. Biomass Detachment. Detachment is implemented in this model only in a simplistic way, with the sole purpose of keeping the floc size within the computational domain. For this goal, all the biomass particles which, because of division or pushing, are located outside a "detachment radius" R_{det} are removed from the floc. The removed particles are not relocated but merely considered lost.

6. Mass Balances of Soluble Substrates in the Floc. The spatial distribution ("the field") of concentrations of a given set of substrates influences the growth rate of a particular biomass type. Conversely, the spatial distribution of bacterial activity affects the substrate concentration fields. Due to growth, division, spreading, attachment, and detachment, the spatial distribution of biomass varies in time. This causes a temporal variation of the substrate fields as well. For this reason, equations of dynamic state diffusion-reaction mass balances must be written for each of n substrates in the subdomain Ω_2:

$$\frac{\partial C_{S,n}}{\partial t} = D_n\left(\frac{\partial^2 C_{S,n}}{\partial x^2} + \frac{\partial^2 C_{S,n}}{\partial y^2} + \frac{\partial^2 C_{S,n}}{\partial z^2}\right) + r_{S,n} \tag{4}$$

TABLE 1. Model Parameters

parameter	symbol	value	units
geometry:			
physical system dimensions	L	800	μm
maximum floc radius	$R_{F,\max}$	375	μm
carrier radius	R_C	100	μm
biomass parameters:			
initial particle biomass	m_0	3×10^{-11}	gCOD/particle
maximum particle biomass	M_X	6×10^{-11}	gCOD/particle
maximum biomass density of particles	ρ_X	60000	gCOD m^{-3}
number of initial biomass particles:			
floc-forming bacteria	$N_{P,0}^{FF}$	25	particles
filamentous bacteria	$N_{P,0}^{FL}$	5	particles
fraction of particles attached:			
floc-forming bacteria	$f_{FF}^{(att)}$	0.2	particles attached/ particles newly formed
filamentous bacteria	$f_{FL}^{(att)}$	0.2	particles attached/ particles newly formed
shoving parameter	k	1	-
maximum specific growth rate	$\mu_{\max}$	6, 10, and 24	day^{-1}
saturation constant for oxygen	$K_{S,O2}$	0.5	gO_2 m^{-3}
saturation constant for organic substrate	$K_{S,S}$	4	gCOD m^{-3}
yield on substrate	Y_{SX}	0.5	gCOD $gCOD^{-1}$
mass transfer parameters:			
oxygen diffusion coefficient	D_{O2}	$1.1'10^{-4}$	m^2 day^{-1}
acetate diffusion coefficient	D_S	$0.4'10^{-4}$	m^2 day^{-1}
boundary layer minimum thickness	δ_{BL}	50	mm
concentrations in bulk liquid			
oxygen	$C_{S,O2}^{(b)}$	0.2 and 1.5	gO_2 m^{-3}
acetate	$C_{S,S}^{(b)}$	20	gCOD m^{-3}
numerical solution parameters:			
grid dimensions for mass balances	N	33	grid nodes
time step	Δt	0.5	h

TABLE 2. Stoichiometric Matrix and Process Rates Used in the Model

	component				
	soluble substrates		microorganisms		process rate
process	C_{S,O_2} $gO_2 \cdot m^{-3}$	$C_{S,S}$ $gCOD \cdot m^{-3}$	$C_{X,FF}$ $gCOD \cdot m^{-3}$	$C_{X,FL}$ $gCOD \cdot m^{-3}$	$gCOD \cdot m^{-3} \cdot day^{-1}$
			Floc-Forming Microorganism, *FF*		
1. growth	$-(1 - Y_{SX})/Y_{SX}$	$-(1/Y_{SX})$	1	0	$\mu_{\max}\{C_{S,S}/(C_{S,S} + K_{S,S})\}\{C_{S,O_2}/(C_{S,O_2} + K_{S,O_2})\}C_{X,FF}$
			Filamentous Microorganism, *FL*		
2. growth	$-(1 - Y_{SX})/Y_{SX}$	$-(1/Y_{SX})$	1	0	$\mu_{\max}\{C_{S,S}/(C_{S,S} + K_{S,S})\}\{C_{S,O_2}/(C_{S,O_2} + K_{S,O_2})\}C_{X,FL}$

In this study, $n = 1$ for oxygen and $n = 2$ for soluble organic carbon. In eq 4 $r_{S,n}$ is the net reaction rate and D_n *is* the effective diffusivity of substrate n in the floc. The left-hand side temporal derivative is the rate of substrate accumulation. The right-hand side contains the isotropic 3-D diffusion rate, with uniform diffusivity all over the place. The net reaction rate is the algebraic sum of the rates of all individual processes that produce or consume that specific substrate.

Because concentrations are considered constant in time and uniform in space in the bulk liquid subdomain Ω_1, the mass balance equations do not need to be solved in Ω_1. The boundary conditions for eq 4 solved in the diffusional subdomain Ω_2 consist of constant substrate concentrations at the floc/bulk liquid interface

$$C_{S,n}^{(R \geq R_{BL})} = C_{S,n}^{(b)} \quad \text{with } R = \sqrt{(x - x_c)^2 + (y - y_c)^2 + (z - z_c)^2} \quad (5)$$

where (x_c, y_c, z_c) is the position of the center of the floc in the computational domain.

The floc radius $R_F(t)$ increases as the floc develops in time and therefore $R_{BL}(t) = R_F(t) + \delta_{BL}$ increases accordingly. For the initial state at $t = 0$, a uniform distribution of concentrations $C_{S,n}^{(x,y,z)} = C_{S,n}^{(b)}$ throughout the whole domain was assumed.

Solution Method. Solution methods for this type of model equations were described in detail in ref *21*. Only the general succession of steps is presented here. After inoculation with a few biomass particles in the middle of the computational domain, the field of substrate concentrations at steady state $C_{S,n}^{(x,y,z)}(t)$ is computed from eqs 4 and 5. A uniform space discretization in N^3 cubic elements of size $h = L/(N\text{-}1)$ is used (Figure 1). The biomass concentration in each cubic element ($C_{X,b}^{(x,y,z)}(t)$) is needed to evaluate the reaction term in eq 4. This is computed from the sum of all biomass particles having the center situated in the cube, divided by the volume h^3. The concentration fields are used for the solution of biomass balances (*2*) for each particle, which are integrated directly for one time step Δt to find $m_{X,b}^{(p)}(t + \Delta t)$. Division of biomass is executed for those particles which mass exceeds the threshold, i.e., when $m_{X,b}^{(p)}(t + \Delta t) > M_X$. Spreading according to the shoving mechanism already described is then necessary, followed by the attachment of new particles. After some of the particles are removed in the detachment step, the biomass dynamics in the time interval Δt has been completed, and a new substrate field needs to be computed.

TABLE 3. Simulated Scenarios

scenario	only floc-former with carrier (cases C)	floc-former and filament without carrier (cases A and B)	
$\mu_{max} = 24\ day^{-1}$			
without attachment			
high $C^{(b)}_{S,O_2}$ (1.5 mg $O_2\,L^{-1}$)	C1	A1	B1
low $C^{(b)}_{S,O_2}$ (0.2 mg $O_2\,L^{-1}$)	C2	A2	B2
with attachment			
high $C^{(b)}_{S,O_2}$ (1.5 mg $O_2\,L^{-1}$)		A3	B3
low $C^{(b)}_{S,O_2}$ (0.2 mg $O_2\,L^{-1}$)		A4	B4
$\mu_{max} = 10\ day^{-1}$			
without attachment			
low $C^{(b)}_{S,O_2}$ (0.2 mg $O_2\,L^{-1}$)		A5	B5
with attachment			
low $C^{(b)}_{S,O_2}$ (0.2 mg $O_2\,L^{-1}$)		A6	B6
$\mu_{max} = 6\ day^{-1}$			
without attachment			
low $C^{(b)}_{S,O_2}$ (0.2 mg $O_2\,L^{-1}$)		A7	B7
with attachment			
low $C^{(b)}_{S,O_2}$ (0.2 mg $O_2\,L^{-1}$)		A8	B8

Case Studies. A mixed culture of floc-forming and filamentous bacterial morphotypes fed with a soluble organic substrate (e.g., acetate, represented in the model as COD) in fully aerobic conditions has been considered. Dissolved oxygen (DO) and organic substrate (COD) are considered the only rate-limiting substrates. The rate equations for bacterial growth and substrate utilization are of Monod type with double limitation. All model parameters are shown in Table 1. The stoichiometry matrix and kinetics expressions used in the model are summarized in Table 2. We were especially interested in the potencial role of diffusion gradients in the formation of filamentous floc structures; therefore, all stoichiometric and kinetic parameters were considered identical for floc-formers and filaments. Molecular diffusion into the floc was the only transport mechanism of dissolved oxygen and soluble substrate. Three scenarios were selected to evaluate the behavior of the model, with the specific conditions indicated in Table 3. Case A assumes the presence of floc-forming bacteria only. In case B, there are both floc-forming and filamentous bacteria. To study the influence of spatial distribution of inoculum on the subsequent floc structure, in case C the floc-forming bacteria grow on a spherical carrier particle with 200 μm diameter. Three specific growth rates (μ_{max} = 24, 10, and 6 day^{-1}) were tested in case A and B. Case C was only evaluated for the highest growth rate, without attachment, and at high and low dissolved oxygen concentration. Each of cases A and B is subdivided in four subcases when $\mu_{max} = 24\ day^{-1}$, with or without attachment, and at high or low dissolved oxygen concentrations.

Results

In this study a first attempt is made to model the structure formation of activated sludge flocs made of two morphotypes of bacteria—a filamentous and a nonfilamentous bacteria—using the *individual-based modeling* approach at the early stage of floc formation. The main processes initially taken into account were the diffusion, reaction, and growth processes. Attachment process was also evaluated in some simulations. Since kinetics was assumed to be similar for both bacterial morphotypes, the microbial competition was primarily based on morphology and on microgradients of substrate concentration. Movies showing the modeling results will be available on the following Web site: http://

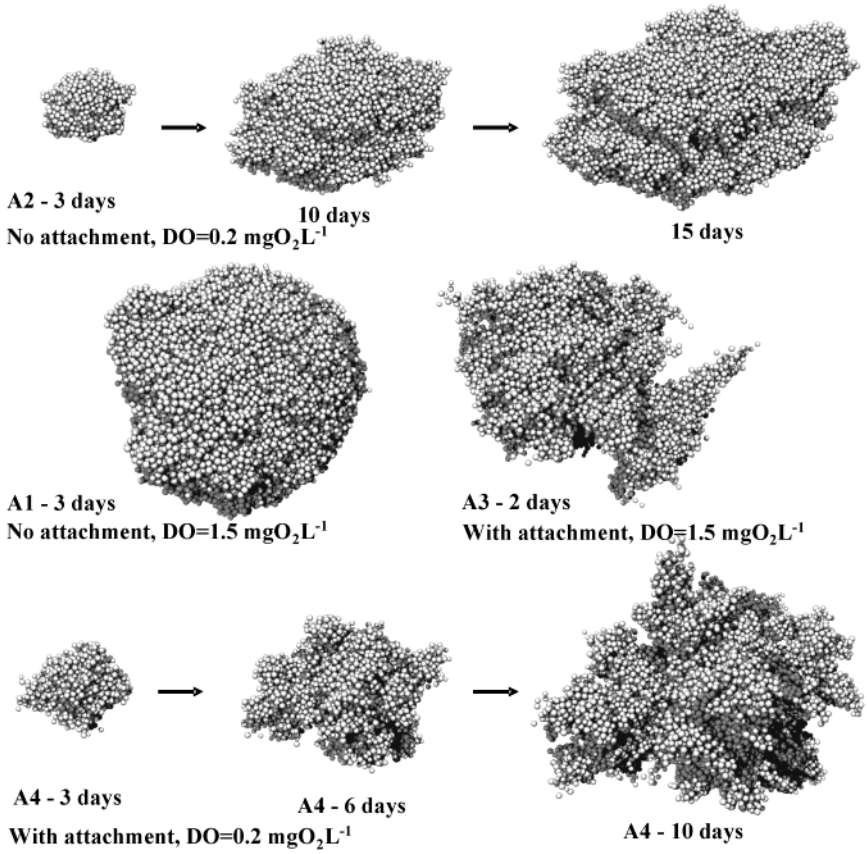

FIGURE 2. Simulated activated-sludge floc with a single morphotype floc-forming bacterium (μ_{max} = 24 day^{-1}) with (cases A3 and A4) or without attachment (cases A1 and A2) at high (cases A1 and A3, 1.5 mg O_2 L^{-1}) and low (cases A2 and A4, 0.2 mg O_2 L^{-1}) dissolved oxygen concentration in the bulk liquid. The size of the final biological floc is approximately 700 μm in diameter.

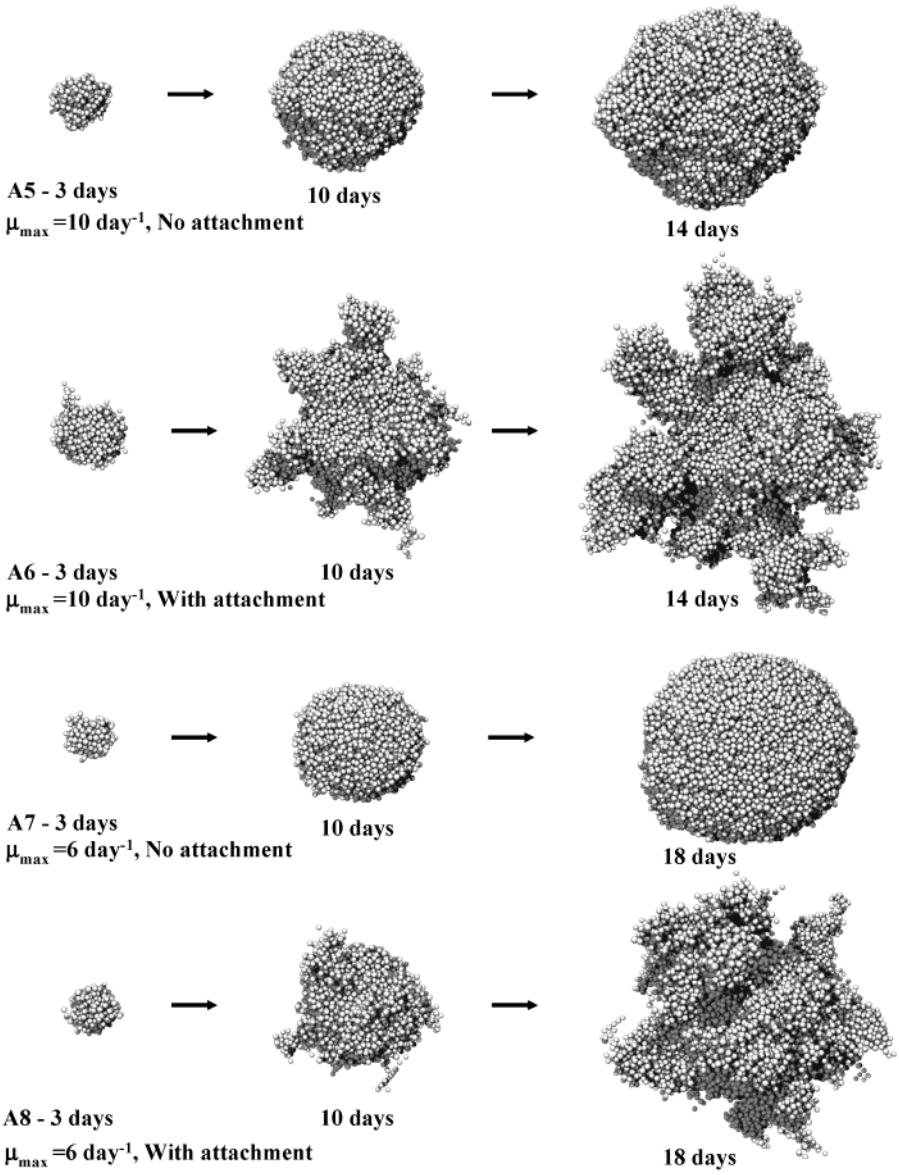

FIGURE 3. Simulated activated-sludge floc with a single morphotype floc-forming bacterium (μ_{max} = 10 day^{-1} in cases A5 and A6; μ_{max} = 6 day^{-1} in cases A7 and A8) with (A6, A8) or without attachment (A5, A7) at low dissolved oxygen concentration in the bulk liquid. The size of the final biological floc is approximately 700 μm in diameter.

www.bt.tudelft.nl/content/ebt/researchgroup_ebt.html and http://www.biofilms.tudelft.nl/.

Floc Development with a Single-Morphotype Floc-Forming Bacterium. The simulated development of an activated sludge floc with a single morphotype floc-forming microorganism, under normal (cases A1 and A3) and low (cases A2 and A4) dissolved oxygen concentration with (cases A3 and A4) or without attachment (cases A1 and A2), at μ_{max} = 24 day^{-1}, is shown in Figure 2. Figure 3 also shows the floc development but at lower specific growth rates (10 and 6 day^{-1}). The evolution of biomass growing on a carrier, without attachment, at high and low $C_{S,O_2}^{(b)}$, is presented in Figure 4.

In the initial stage of floc formation, there is enough substrate in the bulk liquid and the gradients inside the floc are not strong. Therefore, nutrient limitation is not relevant. In these conditions, the floc grows uniformly in all directions, forming a spherical and compact structure (e.g., cases A1 and A2 in Figure 2; cases A5 and A7 in Figure 3).

As the floc gets bigger, and if attachment is not taken into account, two situations can occur. They depend on both specific growth rate and bulk liquid substrate concentration. If there is no substrate limitation (high substrate concentration and/or low specific growth rate, e.g., case A1 in Figure 2 or cases A5 and A7 in Figure 3), then the floc expands uniformly in all the directions and a compact and smoothly shaped floc is obtained. Irregularly shaped flocs are obtained when substrate limitation occurs (e.g., at low dissolved oxygen concentration, case A2 in Figure 2). Biofilms growing on a spherical carrier displayed a similar morphology (case C, Figure 4), which further suggests similarity between activated sludge floc morphogenesis and development of biofilms in particle-based reactors (such as the Biofilm Airlift Suspension or Fluidized Bed systems) under diffusion-limiting conditions.

The irregularity of the floc surface (roughness) increased considerably by including an attachment process (cases A3 and A4). This perturbation of the symmetrical geometry, omnipresent in activated sludge systems and with relevance and magnitude largely unknown, led to the formation of several tips at the floc surface. Even in systems with relatively weak substrate microgradients (case A3 in Figure 2 and Figure 5, and A8 in Figure 3) attachment had a strong effect on floc morphology. These biomass tips develop largely in the direction of the substrate microgradient, growing significantly faster than the biomass inside the floc and leading to the

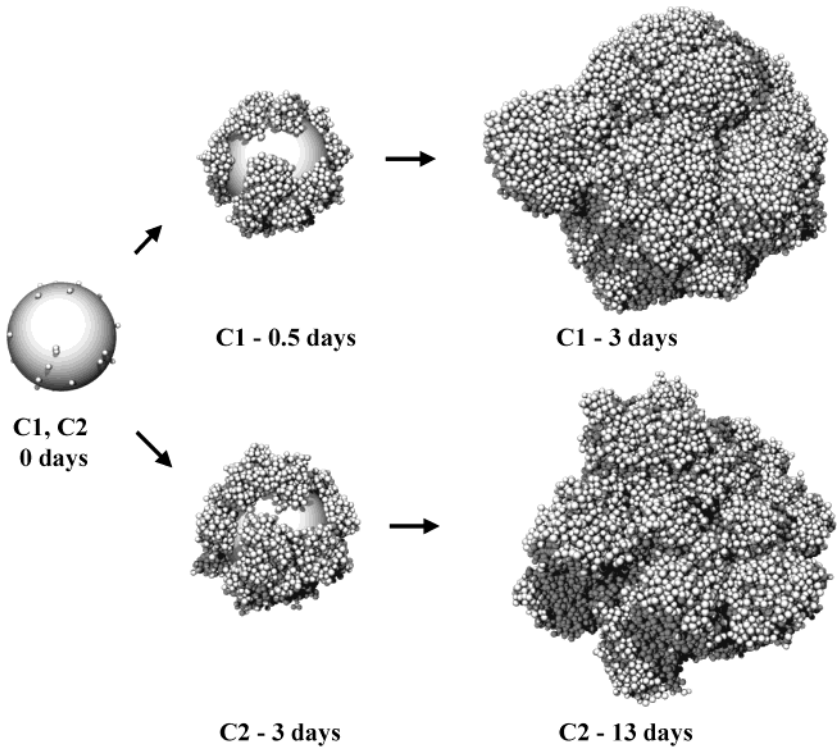

FIGURE 4. Simulated biological aggregate growing on a spherical carrier (200 μm diameter) with a single morphotype floc-forming bacterium without attachment at high (C1, 1.5 mg O_2 L^{-1}) and low (C2, 0.2 mg O_2 L^{-1}) dissolved oxygen concentration. The size of the final aggregate is approximately 700 μm in diameter.

formation of fingerlike structures and, thus, to a more irregularly shaped floc.

Floc Development with a Dual-Morphotype Species: Floc-Forming and Filamentous Bacteria. The development of activated sludge floc with a dual-morphotype floc-forming and filamentous bacteria was simulated under normal (case B3) and low (cases B4, B7, and B8) dissolved oxygen concentration with (cases B3, B4, and B8) or without attachment (case B7).

When attachment is not included in the model, filamentous bacteria quickly reach the border of the activated sludge floc (e.g., case B7 in Figure 6), in either a transport-limited regime or biomass growth-limited regime. Once this happens, filamentous bacteria experience high substrate concentrations and will grow close to the maximum rate. The floc-forming bacteria placed at the floc surface grow with a similar rate, but the overall outward growth velocity of filamentous bacteria is obviously higher because they preferentially grow in only one direction. If no attachment process is considered, filamentous bacteria always grow behind the confines of the floc, dominating the simulated floc structure.

When the microbial growth rate is hardly reduced by substrate limitation (e.g., case B3 in Figure 6) filamentous bacteria quickly reach the border of the activated sludge floc, and, like in the absence of attachment, they protrude from the floc surface and prevail in the competition for space and resources with the floc-forming bacteria. However, in strong substrate-limited regimes (e.g., case B4 in Figure 6—high growth rate and low substrate concentration), few filamentous bacteria protrude from the floc. This is mainly because filaments are just a small fraction of the initial inocula population (about 17%), and as a result of the growth and attachment processes, floc-forming bacteria can rapidly cover them. Under these conditions, filamentous bacteria get less substrate, and although growing predominantly in one or two directions, their overall growth rate is smaller than that of floc-forming bacteria. When the growth rate is smaller, less floc formers will grow and consequently attach to the floc (e.g., case B8 in Figure 6). In these conditions, the filamentous bacteria are exposed to more substrate in the initial stage of the floc development. This availability of substrate together with the typical unidirectional growth gives to the filamentous bacteria competitive advantages, and they will be expected to predominate.

Discussion

The model introduced in this study is, of course, a simplification of the complex reality, and it does not seek to describe all networks of complex biological and physical interactions occurring in activated sludge flocs. The purpose of the developed model was merely to offer a rational platform for the investigation of the morphology of activated sludge flocs and of the competition between floc-forming and filamentous bacteria based mainly on bacterial morphology, cell attachment, and substrate gradients in the floc. The aim of this modeling study was rather to illustrate the phenomena and basic principles (e.g., diffusion limited environments, unidirectional growth, etc.) influencing formation of floc morphology than to develop a fully accurate and calibrated model.

Modeling Results in the Context of the Diffusion-Based Hypothesis. It has been hypothesized that the presence of substrate microgradients inside activated sludge flocs (due to diffusion, reaction, and growth processes) together with the bacterial morphology (i.e., floc-forming bacteria grow in three directions and filamentous bacteria have a predominant unidirectional growth) determine the floc structure (*9*−*11*). In growth-limited systems the substrate gradients inside biological flocs are relatively small, and there is only slight limitation on the microbial growth rate due to substrate diffusion. In these conditions the biological flocs have a smooth shaped surface, and filamentous bacteria are thought to remain mostly inside the floc. In the presence of substrate diffusion limitation the substrate gradients are stronger, and the flocs have an irregular texture, exhibiting fingerlike structures on the surface. Filamentous bacteria are dominant in these conditions since they have an overall higher outward growth vel-

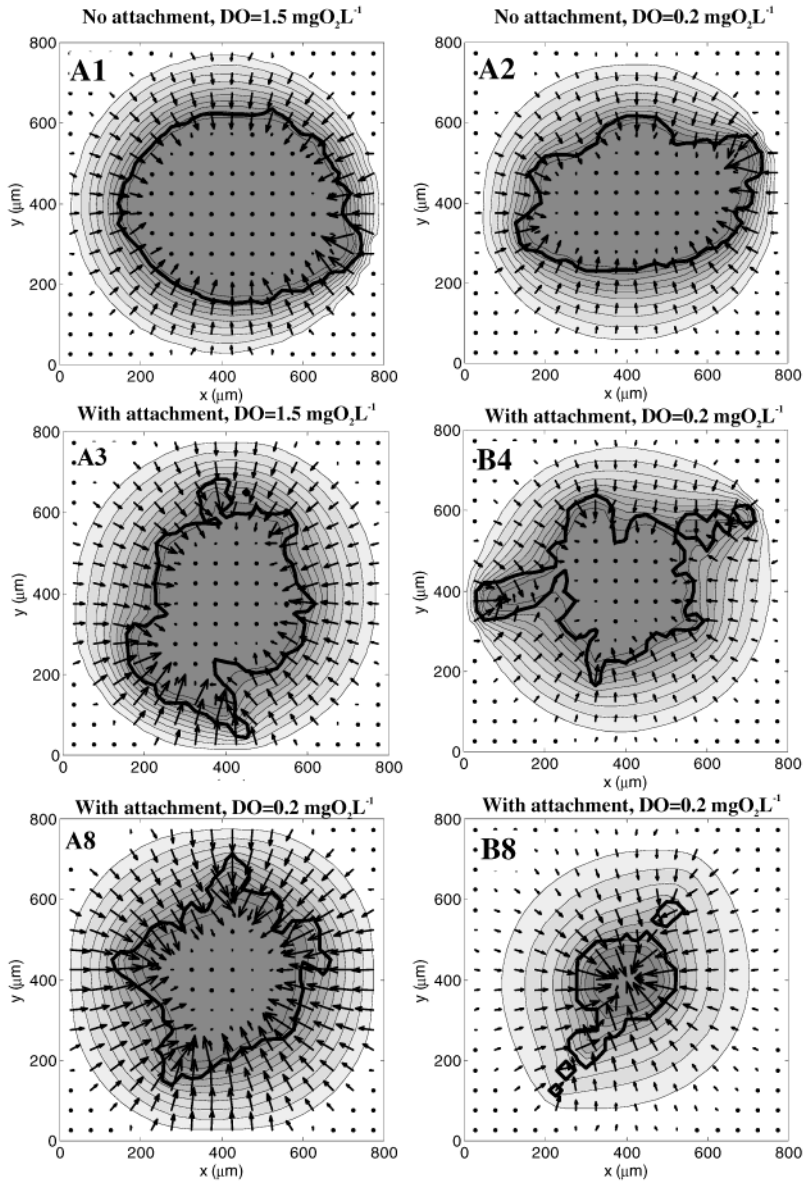

FIGURE 5. Oxygen fluxes (indicated by the length and direction of the arrows) and two-dimensional oxygen concentration fields (darker contour patches indicate lower concentrations) in slices cut through the middle of the floc in cases A1, A2, A3, A8, B4, and B8. Thick lines indicate the floc surface.

ocity. The filaments are expected to protrude from the floc surface and to form a network of filamentous bacteria in the bulk liquid, leading, eventually, to a state of filamentous bulking sludge.

The floc model gives results that are partially in agreement with this hypothesis. For instance, in substrate-limited environments (e.g., in a transport-limited regime) biological flocs with fingerlike structures at the surface were dominant. When the substrate gradients were weaker in the floc, i.e., growth-limited system, and no microbial attachment was considered, tips protruding from the floc surface were not observed, and the floc had a smooth and spherical shape. These modeling results are in line with the experimental observations where regularly shaped and compact flocs are usually dominant in systems without substrate diffusion limitation, e.g., high electron donor and electron acceptor concentrations or vice versa (*9*−*11*), and, thus, with the diffusion-based selection theory. Bacterial structures with similar morphology were also observed in biofilm systems and in colonies formed on agar plates, and their formation was also successfully modeled by several modeling techniques (the approach is always the same: reaction−diffusion processes) (*17*, *23*, *25*−*27*).

However, when filamentous bacteria were present the model could not describe qualitatively some experimental observations and did not follow completely what has been, experimentally based, hypothesized. Although the model predicts that filamentous bacteria predominated, as expected, in transport-limited regimes, their dominance in substrate-rich environments is unrealistic. The simplistic way to make the model work for this particular case would be to assign to the filamentous bacteria a lower specific growth rate at high substrate concentrations, as in the kinetic selection theory (*8*). Some of the drawbacks of this theory were already mentioned before and were discussed in more detail elsewhere (e.g., refs *11*, *28*, and *29*). We believe that other reasons, not incorporated at this stage in the model, may contribute to the nonproliferation of filamentous bacteria (in the bulk liquid) at high substrate concentrations. For instance, it is known that some filamentous bacteria can change morphology in response to changes in environmental conditions (*30*, *31*). It has been reported that when the feeding pattern is a pulse feed (leading to the absence of substrate diffusion limitation) filamentous bacteria are placed mostly around the floc instead of protruding straight from the floc

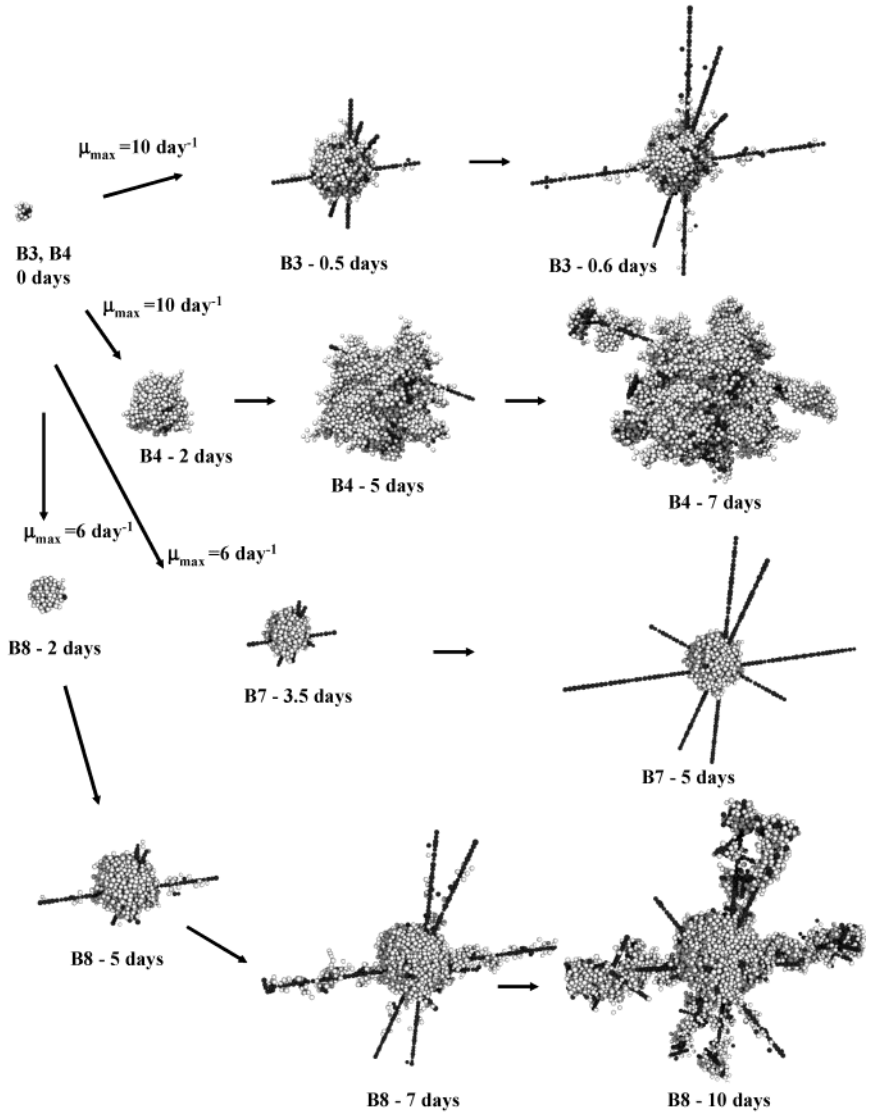

FIGURE 6. Simulated activated-sludge floc with dual-morphotype bacteria (μ_{max} = 10 day^{-1} in cases B3 and B4 and μ_{max} = 6 day^{-1} in cases B7 and B8) with (cases B3, B4, and B8) or without attachment (case B7) at high (case B3) and low dissolved oxygen concentration (cases B4, B7, and B8). In this visualization of the simulated floc morphology, floc-forming biomass is represented by white balls and filamentous biomass by dark balls.

surface, as it occurs in continuously fed completely mixed flow reactor (CMFR) systems (*9*, *10*). Furthermore, filamentous bacteria quickly became dominant when the feeding pattern was changed again to completely mixed regime, indicating that they remained present in the floc interior. With the development of advanced microscopic techniques and molecular tools such as fluorescent in situ hybridization (FISH) bacterial morphology should be studied more in detail, specially under different environmental conditions (e.g., CMFR and plug-flow systems, with feast and famine periods), such as performed recently by Liao et al. (*16*).

Effect of Attachment. The present model suggests that continuous attachment of biomass particles to the floc has a very strong effect on floc structure. The introduction of this perturbation of an otherwise smooth surface led to the formation of tips at the floc surface. These bacterial protrusions have competitive advantages because they have access to substrate-rich environments. They grow faster and mostly in the direction of the substrate gradient, leading to a more open and geometrically irregular floc structure. Modeling results in biofilm systems suggest that there is a minimum spatial perturbation scale that can lead to fingering in these systems (*32*). We did not try to determine the minimum attachment rate that could lead to the formation of the fingerlike flocs. However, the attachment rate used was clearly high enough to disturb the system. Other perturbations, like detachment, floc break-up, and the effect of fluid dynamics, poorly understood and with lack of experimental information, may also play an important role and should be further evaluated. Having a high outward growth velocity, filamentous microorganisms expand faster than floc-forming bacteria and can form a "backbone structure" (*12*, *15*) suitable for adhesion of other cells. Model simulations performed in this study clearly show that both aspects, bacterial morphology and growth in the direction of the substrate gradient (diffusion based process), enhanced by perturbation phenomena such as microbial attachment, are important modeling aspects to be taken into consideration when explaining formation of filamentous floc structures. Moreover, these modeling results suggest that activated sludge flocs and biofilms might be different manifestations of the same phenomena.

Acknowledgments

António Martins received financial support from the Portuguese State in the context of PRAXIS XXI by the Doctoral Scholarship BD/19538/99.

Literature Cited

(1) Mueller, J.; Boyle, W. C.; Lightfoot, E. N. Oxygen diffusion through zoogloeal flocs. *Biotechnol. Bioeng.* **1969**, *10*, 331−358.

(2) Beccari, M.; Di Pinto, A. C.; Ramadori, R.; Tomei, M. C. Effect of dissolved oxygen and diffusion resistances on nitrification kinetics. *Water Res.* **1992**, *26* (8), 1099−1104.

(3) De Beer, D.; Schramm, A.; Santegoeds, C. M.; Nielsen, H. K. Anaerobic processes in activated sludge. *Water Sci. Technol.* **1998**, *37* (4−5), 605−608.

(4) Schramm, A.; Santegoeds, C. M.; Nielsen, H. K.; Wagner, M.; Pribyl, M.; Wanner, J.; Amann, R.; de Beer, D. On the occurrence of anoxic microniches, denitrification, and sulfate reduction in aerated activated sludge. *Appl. Environ. Microbiol.* **1999**, *65* (9), 4189−4196.

(5) Merchuk, J. C.; Asenjo, J. A. Communication to the Editor: The Monod equation and mass transfer. *Biotechnol. Bioeng.* **1995**, *45* (1), 91−94.

(6) Kappeler, J.; Gujer, W. Development of a mathematical model for aerobic bulking. *Water Res.* **1994**, *28* (2), 303−310.

(7) Pérez, J.; Picioreanu, C.; van Loosdrecht; M. C. M. Modeling biofilm and floc diffusion processes based on analytical solution of reaction−diffusion equations. *Water Res.* **2003**, in press.

(8) Chudoba, J.; Grau, P.; Ottová, V. Control of activated sludge filamentous bulking − II. Selection of microorganisms by means of a selector. *Water Res.* **1973**, *7*, 1389−1406.

(9) Martins, A. M. P.; van Loosdrecht, M. C. M.; Heijnen, J. J. Effect of feeding pattern and storage on the sludge settleability under aerobic conditions. *Water Res.* **2003**, *37(11)*, 2555−2570.

(10) Martins, A. M. P.; van Loosdrecht, M. C. M.; Heijnen, J. J. *Appl. Microbiol. Biotechnol.* **2003**, *62(5−6)*, 586−593.

(11) Martins, A. M. P.; Pagilla, K.; van Loosdrecht, M. C. M.; Heijnen, J. J. Filamentous bulking sludge − a critical review. *Water Res.* **2004**, *38(4)*, 793−817.

(12) Sezgin, M.; Jenkins, D.; Parker, D. S. A unified theory of filamentous activated sludge bulking. *J. Water Pollut. Control Fed.* **1978**, *50* (2), 362−381.

(13) Lau, O. A.; Strom, P. F.; Jenkins, D. Growth kinetics of *Sphaerotilus natans* and a floc former in pure and continuous culture. *J. Water Pollut. Control. Fed.* **1984**, *56*, 41−51.

(14) Urbain, V.; Block, J. C.; Manem, J. Bioflocculation in activated sludge: An analytic approach. *Water Res.* **1993**, *27* (5), 829−838.

(15) Cenens, C.; Smets, I. Y.; van Impe, J. F. Modelling the competition between floc-forming and filamentous bacteria in activated sludge wastewater treatment systems − II. A prototype mathematical model based on kinetic selection and filamentous backbone theory. *Water Res.* **2000**, *34* (9), 2535−2541.

(16) Liao, J.; Lou, I.; de los Reyes III, F. L. Relationship of species-specific filament levels to filamentous bulking in activated sludge. *Appl. Environ. Microbiol.* **2004**, *70* (4), 2420−2428.

(17) Picioreanu, C.; van Loosdrecht, M. C. M.; Heijnen, J. J. Mathematical modelling of biofilm structure with a hybrid differential-discrete cellular automaton approach. *Biotechnol. Bioeng.* **1998**, *58*, 101−116.

(18) Takács, I.; Fleit, E. Modelling of the micromorphology of the activated sludge floc: low DO, low F/M bulking. *Water Sci. Technol.* **1995**, *31* (2), 235−243.

(19) Kreft, J.-U.; Booth, G.; Wimpenny, J. W. T. BacSim, a simulator for individual-based modelling of bacterial colony growth. *Microbiol.* **1998**, *144*, 3275−3287.

(20) Kreft, J.-U.; Picioreanu, C.; Wimpenny, J. W. T.; van Loosdrecht, M. C. M. *Microbiol. SGM* **2001**, *147*, 2897−2912.

(21) Picioreanu, C.; van Loosdrecht, M. C. M. Chapter 22 In *Biofilms in Medicine, Industry and Environmental Biotechnology − Characteristics, Analysis and Control*; Editors: P. Lens, V. O'Flaherty, A. P. Moran, P. Stoodley, T. Mahony, IWA Publishing: May 2003; pp 413−437, ISBN 1843390191.

(22) Picioreanu, C.; Kreft, J.-U.; van Loosdrecht, M. C. M. Particle-based multidimensional multispecies biofilm model. *Appl. Environ. Microbiol.* **2004**, *70* (5), 3024−3040.

(23) Picioreanu, C.; van Loosdrecht, M. C. M.; Heijnen, J. J. Mathematical modelling of biofilm structure with a hybrid differential-discrete cellular automaton approach. *Biotechnol. Bioeng.* **1998**, *58*, 101−116.

(24) Kaye, B. *A random walk through fractal dimensions*; VCH: Weinheim, Germany, 1989; pp 38−53.

(25) Ben-Jacob, E.; Schochet, O.; Tenenbaum, A.; Cohen, I.; Czirok, A.; Vicsek, T. Generic modelling of cooperative growth patterns in bacterial colonies. *Nature* **1994**, *368* (3), 46−49.

(26) Van Loosdrecht, M. C. M.; Eikelboom D.; Gjaltema, A.; Mulder, A.; Tijhuis, L.; Heijnen, J. J. Biofilm structures. *Water Sci. Technol.* **1995**, *32* (8), 35−43.

(27) Wimpenny, J. W. T.; Colasanti, R. A unifying hypothesis for the structure of microbial biofilms based on cellular automaton models. *FEMS Microb. Rev.* **1997**, *22*, 1−16.

(28) Wanner, J. *Activated Sludge Bulking and Foaming Control*; Technomic Publishing Co. Inc.: Lancaster, PA, 1994.

(29) Seviour, R. J.; Blackall, L. L. *The Microbiology of Activated Sludge*; Kluwer: Dordrecht, 1999.

(30) Buali, A. M.; Horan, N. J. Variable morphology in certain filamentous bacteria and implications of this for theories of activated sludge bulking. *Environ. Technol. Lett.* **1989**, *10*, 941−950.

(31) Seviour, E. M.; Blackall, L. L.; Christensson, C.; Hugenholtz, P.; Cunningham, M. A.; Bradford, D.; Stratton, H. M.; Seviour, R. J. The filamentous morphotype Eikelboom type 1863 is not a single genetic entity. *J. Appl. Microbiol.* **1997**, *82*, 411−421.

(32) Dockery, J.; Klapper, I. Finger Formation in Biofilm Layers. *SIAM J. Appl. Math.* **2001**. *62* (3), 853−869.

Received for review March 3, 2004. Revised manuscript received August 16, 2004. Accepted August 18, 2004.

ES049659L